

Technical report 23-006

# A Novel Mechanistic Modelling Approach for Microbial Selection Dynamics: Towards Improved Design and Control of Raceway Reactors for Purple Bacteria\*

A. Alloul, A. Moradvandi, D. Puyol, R. Molina, G. Gardella,  
S. E. Vlaeminck, B. De Schutter, E. Abraham, R. E. F. Lindeboom,  
and D. G. Weissbrodt

*To cite this work, please refer to the published version:*

A. Alloul, A. Moradvandi, D. Puyol, R. Molina, G. Gardella, S. E. Vlaeminck, B. De Schutter, E. Abraham, R. E. F. Lindeboom, and D. G. Weissbrodt, "A novel mechanistic modelling approach for microbial selection dynamics: Towards improved design and control of raceway reactors for purple bacteria," *Bioresource Technology*, vol. 390, p. 129844, Dec. 2023. doi:[10.1016/j.biortech.2023.129844](https://doi.org/10.1016/j.biortech.2023.129844)

# A novel mechanistic modelling approach for microbial selection dynamics: towards improved design and control of raceway reactors for purple bacteria

Abbas Alloul<sup>a,c,1</sup>, Ali Moradvandi<sup>b,f,1,\*</sup>, Daniel Puyol<sup>d</sup>, Raúl Molina<sup>d</sup>, Giorgio Gardella<sup>b</sup>, Siegfried E. Vlaeminck<sup>a</sup>, Bart De Schutter<sup>f</sup>, Edo Abraham<sup>b</sup>, Ralph E. F. Lindeboom<sup>b</sup>, David G. Weissbrodt<sup>c,e</sup>

<sup>a</sup>*Research Group of Sustainable Energy, Air and Water Technology, Department of Bioscience Engineering, University of Antwerp, Groenenborgerlaan 171, 2020, Antwerpen, Belgium*

<sup>b</sup>*Department of Water Management, Delft University of Technology, Mekelweg 5, 2628 CD, Delft, The Netherlands*

<sup>c</sup>*Department of Biotechnology, Delft University of Technology, Maasweg 9, Delft, 2629 HZ, The Netherlands*

<sup>d</sup>*Group of Chemical and Environmental Engineering, University Rey Juan Carlos, 28933, Madrid, Spain*

<sup>e</sup>*Department of Biotechnology and Food Science, Norwegian University of Science and Technology, 7034, Trondheim, Norway*

<sup>f</sup>*Delft Center for Systems and Control, Delft University of Technology, Mekelweg 2, 2628 CD, Delft, The Netherlands*

---

## Abstract

Purple phototrophic bacteria (PPB) show an underexplored potential for resource recovery from wastewater. Raceway reactors offer a more affordable full-scale solution on wastewater and enable useful additional aerobic processes. Current mathematical models of PPB systems provide useful mechanistic insights, but do not represent the full metabolic versatility of PPB and thus require further advancement to simulate the process for technology development and control. In this study, a new modelling approach for PPB that integrates the photoheterotrophic, and both anaerobic and aerobic chemoheterotrophic metabolic pathways through an empirical parallel metabolic growth constant was proposed. It aimed the modelling of microbial selection dynamics in competition with aerobic and anaerobic microbial community under different operational scenarios. A sensitivity analysis was carried out to identify the most influential parameters within the model and calibrate them based on experimental data. Process perturbation scenarios were simulated, which showed a good performance of the model.

*Keywords:* bio-process modelling, process design, physico-chemical process, resource recovery, purple non-sulphur bacteria.

---

\*Corresponding author: A. Moradvandi: a.moradvandi@tudelft.nl

<sup>1</sup>Abbas Alloul and Ali Moradvandi contributed equally as first author.

## 1. Introduction

Purple phototrophic bacteria (PPB) offer great potential to recover resources from wastewater like organics and the nutrients nitrogen and phosphorus. The phototrophically produced biomass have circular economy applications as microbial fertilizer, biostimulant, animal feed ingredient, and bioplastics feedstock (Alloul et al., 2023; Capson-Tojo et al., 2020). PPB exhibit metabolic diversity and versatility, capable of thriving on various energy sources (photo- and chemotrophy), electron sources (organo- and lithotrophy), and carbon sources (auto- and heterotrophy) (Imhoff, 2006). As phototrophs, they have the unique ability to grow on infrared light, are anoxygenic and proliferate swiftly in anaerobic mixed-culture systems fed with volatile fatty acids (VFAs). For wastewater treatment and resource recovery, this photoorganoheterotrophic mode is mostly studied (Capson-Tojo et al., 2020).

In research labs, membrane (photo)bioreactors, tubular photobioreactors, flat-plate photobioreactors, as well as stirred-tank photobioreactors have been mainly used to achieve high PPB selectivity (Alloul et al., 2021a; Capson-Tojo et al., 2020; Cerruti et al., 2020; Hülsen et al., 2022). Successful selection of PPB has been mainly obtained in closed configurations to maintain an anaerobic reactor environment. However, the high capital expenditure of these systems may prevent implementation at full scale (Acién et al., 2012; Alloul et al., 2021a). Open raceway reactors reduced total investment and operational cost 5 to 10-fold, relative to closed anaerobic photobioreactors (Alloul et al., 2021a). However, open raceway ponds are exposed to passive oxygenation ( $217\text{--}226\text{mgO}_2\text{L}^{-1}\text{h}^{-1}$ ) through the combination of the paddle wheel rotation used to circulate the wastewater and their high atmospheric surface-to-volume ratio used to maximize light accessibility ( $5\text{m}^2\text{m}^{-3}$ ). The uncontrolled supply of dissolved oxygen in this system not only enables aerobic conversions but also creates a competitive environment where PPB compete with aerobic bacteria (AEB) for available organic substrates that may be contaminated by external bacteria (Alloul et al., 2021a). Achieving high PPB selectivity is, therefore, more challenging than in closed anaerobic systems. Nonetheless, changing the operational conditions in terms of oxygen supply, light availability, sludge retention time (SRT), and chemical oxygen demand (COD) loading successfully boosted the PPB abundance from 14% to 78% in a 100-L raceway reactor operated on synthetic wastewater (Alloul et al., 2021a).

Mechanistic simulation models are needed to improve the design and operation of PPB processes, boost piloting activities, scale up implementations, and control the processes. On a more fundamental basis, genome-scale metabolic models have been developed to describe biohydrogen production in pure-culture systems (Golomysova et al., 2010; Imam et al., 2011); however, they cannot be directly used for environmental biotechnology applications. Puyol et al. (2017) have translated the activated sludge model formalism to predict nutrient conversions driven by PPB, which has been discussed by Henze et al. (2015). The Photo-anaerobic model (PAnM) is limited to photo-anaerobic conditions and does not take microbial competition with non-PPB guilds like aerobic and fermentative chemoorganoheterotrophs and photolithoautotrophs into account. The extended version of PAnM (ePAnM) has been proposed by (Capson-Tojo et al., 2023), which integrates eight different types of microorganisms, i.e. PPB, AEB, acidogenic and acetogenic fermenters, aerobic predators, heterotrophic

and autotrophic sulphate reducing bacteria, and microalgae and takes diverse metabolic capabilities of PPB into account. Compared to PAnM, PPB photoheterotrophic, aerobic and anaerobic uptake rates and yields have been used to simulate PPB growth in batch and semicontinuous processes in the ePAnM. As far as observed, the difference in maximum growth rate in relation to PPBs metabolic versatility under various environmental conditions were not explicitly addressed Puyol et al. (2017); Capson-Tojo et al. (2023). While the ePAnM is capable of adapting to various environmental conditions, it has been suggested recalibrating specifically for the operation of open pond raceway reactors (Capson-Tojo et al., 2023), which was investigated in this study. A detailed comparison between the structures of the PAnM, the ePAnM, and the PBM model can be found in a table in the supplementary material (see supplementary material). With the technological development of PPB raceway systems, a more comprehensive model is necessary to simulate wastewater treatment along with microbial selection to assess operational and control scenarios for raceway reactors and also taking parallel metabolic growth into account. Such a model will allow to better engineer, implement, and control raceway reactors by predicting process conditions, variations, and perturbations that affect the PPB abundance and the treatment performance.

In this study, a new mechanistic purple bacterial model (PBM) was constructed that considers the most relevant metabolic growth modes that PPB and competing microbes including aerobic and anaerobic heterotrophic bacteria within a raceway reactor for the purpose of process simulation. This study introduced a novel approach aimed at incorporating diverse growth pathways of PPB, considering their simultaneous occurrence by hypothesizing a phenomenon observed in previous research—namely, the coexistence of multiple growth pathways. Therefore, an empirical parallel metabolic growth constant was defined to account for the contribution of alternative pathways to PPB growth alongside the dominant pathway. After model construction, a sensitivity analysis was conducted to identify the most influential parameters and to assess the impact of parameter variations on the model outputs. Calibration of the important factors was carried out through iterative error minimization. Short- and long-term perturbations of incoming soluble organic matters, volatile fatty acid (VFA), suspended solids and light variations were simulated to their effects on PPB abundance and COD removal rate.

## 2. Materials and methods

### 2.1. Model description

The PBM was constructed to simulate the wastewater treatment performance and PPB selectivity in open raceway reactors for design and control purposes. The PBM can be transferred to other reactor systems or used as add-on to existing models such as the Activated Sludge Model (ASM), Anaerobic Digestion Model no.1 (ADMn1) or algae-bacteria models e.g., the ALBA model (Batstone et al., 2002; Henze et al., 2015; Casagli et al., 2021), since the PBM is units compatible to the ASM and ADMn1 series of the International Water Association (IWA). The PBM consists of 15 state variables with 3 state variables associated with PPB community, and 16 processes including 12 biological and 4 physical processes.

### 2.1.1. State variables, balances, and processes

In this section, the structure of the proposed PBM model is explained by describing state variables, balances, and biological and physical processes. The PBM state variables are summarized in Table 1, and biological and physical processes described in Table 2. Moreover, the PBM Peterson matrix and the parameters' values are provided in the supplementary material (see supplementary material).

*Microbial community:* The microbial biomass were divided in three main categories, namely purple phototrophic bacteria (PPB), aerobic bacteria (AEB) and anaerobic bacteria (ANB), reflecting the main microbial groups thriving in a raceway reactor covered with a selective infrared cover operated on COD-rich wastewater (Alloul et al., 2021a). The PPB-based bacteria were also divided into three subgroups consisted of photoheterotrophic grown PPB ( $X_{PB,ph}$ ), aerobic chemoheterotrophic grown PPB ( $X_{PB,aec}$ ), and anaerobic chemoheterotrophic grown PPB ( $X_{PB,anc}$ ).

*Substrates and products:* The incoming COD consists of both particulate and soluble matters. Readily biodegradable COD was divided in a non-volatile fatty acid ( $S_S$ ) and C2-C6 volatile fatty acid ( $S_{VFA}$ ) fractions. The growth kinetics and biochemical pathways for both substrates are different (Batstone et al., 2002; Puyol et al., 2017). VFAs and other dissolved organics follow a different uptake pattern, and lead to different selections (Cerruti et al., 2023). Furthermore, subdividing soluble solids based on individual VFA might also be reasonable because VFAs induce different maximal specific growth rates, yet might increase complexity, thereby, making the model impractical for wastewater treatment applications. As nutrients, only inorganic nitrogen ( $S_{IN}$ ) and phosphorus ( $S_{IP}$ ) were included, since organic fractions can be hydrolyzed in the preceding fermentation as suggested by Alloul et al. (2021a) for operational functionality of raceway reactors in producing PPB.

Since raceway systems are open reactors, the concentration of dissolved oxygen ( $S_{O_2}$ ) plays an important role, especially since AEB can outcompete PPB. The effect of the paddle wheel on the mass transfer of dissolved oxygen in the liquid phase was also taken into account for modelling. To close carbon, electron and mass balances, the production of carbon dioxide ( $S_{CO_2}$ ) and hydrogen ( $S_{H_2}$ ), which can come from non-VFA and VFAs, were included in the model.

The mentioned biochemical and physical processes take place in the raceway reactor. The lab-scale and even pilot-scale raceway reactors can be modelled as a single continuous-flow stirred tank (CSTR) due to their reduced dimensions and the high water circulation flow. Sequencing batch with cycles of filling the reactor with influent once a day and turning on the paddle wheel to promote gas transfer during the day, and stopping the paddle wheel to slow down the reactions and settle the biomass during nights prior to purging the excess sludge, is assumed as a modelling of the reactor regime to simulate the real situation in physical models in labs. The model can also be used either for other reactor measures by changing volume ( $V$ ) and surface area ( $A$ ) in the model implementation or for other reactor geometry systems such as tubular or flat plate photobioreactors with some modifications to consider biofilm formation. Raceway reactors typically have a liquid depth of 20 cm and a surface-to-volume ratio of  $5 \text{ m}^2 \text{ m}^{-3}$  (Norsker et al., 2011).

*Balances and system dynamics equations:* The reactor volume may be varied

during filling and extracting phases, especially if they are not done at the same time. Its variability, therefore, can be written as a following differential equation:

$$\frac{dV}{dt} = Q_{\text{inflow}}(t) - Q_{\text{outflow}}(t), \quad (1)$$

where,  $V$ ,  $Q_{\text{inflow}}$ ,  $Q_{\text{outflow}}$  denote the reactor volume and the input and output flow rates, respectively. Therefore, the mass balances of the soluble materials can be written as follows:

$$\frac{dS_i}{dt} = \frac{S_i^{\text{input}} Q_{\text{inflow}}(t) - S_i(Q_{\text{outflow}}(t) + \frac{dV}{dt})}{V_0} + \sum v_i \rho_i, \quad (2)$$

where  $V_0$ ,  $v_i$ ,  $\rho_i$  denote the reactor volume and the input and output flow rates, the initial volume, the stoichiometric coefficient, and the process rate of the corresponding conversion, respectively, in which the subscript  $i$  denotes component name.

The mass balances for the particulate materials can be written in a similar way, while integrating a factor related to hydraulic (HRT) and sludge (SRT) retention times to model the effect of the paddle wheel activation, the effluent extraction, and the water recirculation if needed. This factor was defined as the HRT/SRT ratio ( $f_{H/S}$ ) to consider the fraction of removed particles. The HRT/SRT ratio provides insights into the performance and stability of the reactor, which should be optimized. The mass balance equation for particulate materials becomes the following, considering transport and conversion terms:

$$\frac{dX_i}{dt} = \frac{X_i^{\text{input}} Q_{\text{inflow}}(t) - X_i(Q_{\text{outflow}}(t) + \frac{dV}{dt} f_{H/S})}{V_0} + \sum v_i \rho_i. \quad (3)$$

In addition, the mass balance equation of oxygen was modified to take the effect of oxygen dissolution into account when the paddle wheel is working. A switching function associated with the on/off conditions of the paddle wheel was, therefore, integrated to consider oxygen promotion.

*Gas-liquid transfers:* These systems are open to air and agitated with a paddle wheel. Gas-liquid mass transfer of four components, was, therefore, included in the model, namely: oxygen dissolution from the air through paddle wheel rotation; carbon dioxide dissolution from the air or produced through biological processes; hydrogen dissolution from the air or produced through biological processes; and ammonia origination from the incoming wastewater. The mass transfer kinetics for all gases was described through volumetric mass transfer rate and the gas saturation concentration through Henry's law.

*Inhibitory factors:* As for the activated sludge model and anaerobic digestion model, kinetics expressions are multiplicative and based on Monod type functions to describe limitations of organics, ammonium, phosphate, light, and oxygen. In comparison with the PAnM (Puyol et al., 2017) and the ePAnM (Capson-Tojo et al., 2023), since, the PBB community was not considered as a single cell in the PBM, light inhibitory factor is differentiated between photoheterotrophy and chemoheterotrophy. Moreover, different oxygen inhibitions were taken into account for PBB photoheterotrophy and chemoheterotrophy as well as aerobic and anaerobic microbial communities. Competitive inhibition function between VFAs and other soluble organics was also included into the

PBM as PBB growth competition has been reported by (Cerruti et al., 2020).

### 2.1.2. PPB and its competition

*Metabolic versatility of PPB:* Six biological processes were assigned to PPB, namely: two photoheterotrophic growths on soluble organics and VFAs, respectively; two aerobic chemoheterotrophic growths on soluble organics and VFAs, respectively; one anaerobic chemoheterotrophic growth on soluble organics; and biomass decay into biodegradable materials and inerts while releasing inorganic nitrogen, phosphorus and carbon. The PPB biomass therefore comprises grow metabolisms by photoheterotrophy ( $X_{PB,ph}$ ), aerobic chemoheterotrophy ( $X_{PB,aec}$ ), and anaerobic chemoheterotrophy ( $X_{PB,anc}$ ). This subdivision reflects the different types of metabolisms that PPB conduct in a raceway reactor subjected to varying environmental conditions, e.g., availability of light, oxygen, fermentable organics, etc. (Alloul et al., 2021a). The model was written to account for the ability of PPB to grow on different substrates (electron donors and carbon sources) or energy sources (light or chemical redox reactions) in parallel and to hypothesize a combined metabolic-mechanistic understanding to the most opportune metabolism. The parallel metabolic growth of PPB was implemented in the model by introducing a novel factor and inhibition-type functions with light and oxygen to control photoheterotrophy and chemoheterotrophies, respectively. Therefore, besides the light and oxygen inhibition functions, a parallel metabolic growth constant ( $M_S$ ) between the three PPB biomass types was included, so that biomass is grown phototrophically and chemotrophically in parallel during shifting between days and nights. This factor plays a pivotal role in accounting for the contribution of alternative pathways to PPB growth alongside the dominant pathway. This novel factor is the main difference between the PBM proposed and the PAnM and ePAnM developed by (Puyol et al., 2017; Capson-Tojo et al., 2023) and can be written as follows:

$$f_{ph} = X_{PB,ph} + M_S(X_{PB,aec} + X_{PB,anc}) \quad (4a)$$

$$f_{aec} = X_{PB,aec} + M_S(X_{PB,ph} + X_{PB,anc}) \quad (4b)$$

$$f_{anc} = X_{PB,anc} + M_S(X_{PB,ph} + X_{PB,aec}) \quad (4c)$$

where  $f_{ph}$ ,  $f_{aec}$ , and  $f_{anc}$  represents state variables with regard to photoheterotrophic, aerobic chemoheterotrophic, and anaerobic chemoheterotrophic growths, respectively. This constant means that biomass grown photoheterotrophically is able to use chemoheterotrophic conversion and vice versa, which have been experimentally observed by Alloul et al. (2021b); Cerruti et al. (2023). PPB are known to divide their metabolic growth pathways over photo- and chemotrophy. An  $M_S$  of zero implies that PPB biomass grown photoheterotrophically cannot switch to chemoheterotrophy and is, therefore, completely independent of chemoheterotrophy. Without the inclusion and proper calibration of this constant, the model is not able to accurately predict the production of PPB.

*Microbial competitors:* Microbial processes that compete with PPB metabolisms in the raceway biomass are mainly aerobic chemoheterotrophy by AEB and anaerobic chemoheterotrophy by ANB. Nitrifiers, methanogens, denitrifiers and sulfate reducing bacteria were not implemented in the model since not prevalent in open raceway reactors (Alloul et al., 2021a). It should be highlighted that the model structure can be adapted with additional processes (such as described in ASM and ADM) by users, depending on the local conditions to be investigated.

## 2.2. Model analysis

In this section, the methodology employed to analyze the PBM is described. Sensitivity analysis was carried out to first identify the influential parameters of the model, then calibrate these impactful model parameters using data from controlled experiments. The robustness of the model was assessed by simulating the model under different operational scenarios.

### 2.2.1. Sensitivity analysis

After model construction, a local sensitivity analysis was conducted to assess the impact of each parameter on the PBM. The PBM contains various parameters, ranging from physical to kinetic parameters, in which physical parameters and yields have been broadly researched and validated. Total kinetic parameters including maximal specific growth rates ( $\mu_m$ ), substrate affinities ( $K_S$ ), inhibition constants ( $K_I$ ), and specific decay rate ( $b_m$ ) associated with microbial community are covered in the sensitivity analysis, which a part of them is directly linked to PPB.

As baseline, kinetic parameters were obtained from previous researches. The maximal specific and decay rates were given from the activated sludge model (Henze et al., 2015), the ADM1 (Batstone et al., 2002), the PANM (Puyol et al., 2017), and the substrate affinities from Katsuda et al. (2000); Capson-Tojo et al. (2021). Newly-defined parameters, such as PPB oxygen affinities, were chosen based on the experiments (Alloul et al., 2021a), trial and error, as well as the expert knowledge. Therefore, to measure the impact of parameters on the model output, sensitivity functions were computed one-at-the-time (OAT). Each parameter was uniformly perturbed ten times (the sensitivity coefficient) higher and lower of the default values (Manhaeghe et al., 2020). The duration time of each simulation was set to 50 days to ensure reaching the steady-state condition. The relative abundance of PPB, COD removal rate ( $\text{mg COD L}^{-1} \text{d}^{-1}$ ), biomass productivity ( $\text{mg COD L}^{-1} \text{d}^{-1}$ ) and biomass yield ( $\text{mg COD biomass mg}^{-1} \text{COD removed}$ ) were selected as outputs because of their feasibility to measure for the experiments. The mean of the model output for the last five days (when the process reaches steady-state) for each iteration was calculated, and to be able to compare the sensitivity functions, the absolute sensitivity should be converted into relative sensitivity by dividing the output results by the baseline (default values). Therefore, the outcome can be compared between parameters and outputs. The wastewater composition for the sensitivity analysis was considered based on the synthetic medium proposed by Alloul et al. (2021a).

### 2.2.2. Overview of the experiments

Based on operational strategies to selectively produce PPB raceway reactors discussed by Alloul et al. (2021a), three scenarios were selected as (i) 24 h stirring at a surface-to-volume ratio of  $5 \text{ m}^2 \text{ m}^{-3}$  with a 12 h light and 12 h dark regime (scenario 1), (ii) 12 h stirring during the light period at a surface-to-volume ratio of  $5 \text{ m}^2 \text{ m}^{-3}$  with a 12 h light and 12 h dark regime (scenario 2), (iii) 24 h stirring at a surface-to-volume ratio of  $10 \text{ m}^2 \text{ m}^{-3}$  with a 12 h light and 12 h dark regime (scenario 3).

These three controlled experiment were conducted in a 100-L pilot scale raceway reactor with a mixed PPB culture dominated by *Rhodobacter capsulatus* and a *Rhodospseudomonas* (Alloul et al., 2021a). The reactor has been

operated for 40 days on synthetic wastewater at a temperature of 28 °C and illuminated artificially with halogen lamps (50 W m<sup>-2</sup>). The raceway had a depth of 10–20 cm and a surface-to-volume ratio of 5–10 m<sup>2</sup> m<sup>-3</sup>. A VFAs solution was used as substrate composed by acetate, propionate and butyrate in a ratio of 1/1/1 gCODL<sup>-1</sup>. All experiments started with a volatile suspended solid (VSS) concentration of 0.02 gVSSL<sup>-1</sup>. The initial and final total COD and soluble COD were measured in order to analyze the COD removal, final biomass and yield of the reactions. Moreover, optical density at 660 nm (OD660) was measured to extrapolate growth. The ratio between absorbance (A660) and TSS was also taken from (Cerruti et al., 2020). The focus was on measuring PPB abundance, which aligns with practical feasibility.

### 2.2.3. Calibration and validation

A relevant range for each of selected parameters was selected based on expert knowledge and sensitivity analysis to be calibrated. All possible combinations of the five parameters were then computed for the three mentioned operational strategies. The mean of the last five simulated days when the process reaches steady-state was, then, calculated for each iteration of every individual outputs, i.e. relative abundance of PPB, COD removal rate, biomass productivity and biomass yield. Therefore, the relative error ( $e_{rel}$ ) was calculated as the absolute difference between the simulation and the experiment divided by the experimental value, given as follows:

$$e_{rel} = \frac{|y^{\text{simulation}} - y^{\text{experiment}}|}{y^{\text{experiment}}}, \quad (5)$$

where,  $y^{\text{simulation}}$  and  $y^{\text{experiment}}$  denote each of the mentioned outputs from the simulation and experiment, respectively. This was achieved by implementing a nested loop structure using the “for” programming construct to identify a parameters’ combination that exhibited the lowest relative error for each model output, while also demonstrating a consistent trend across the three strategies. This procedure led to find the calibrated parameters, while assessing the model performance with the relative error as summarized in Table 4.

### 2.2.4. Perturbed scenario assessment

The calibrated model can be used to improve the design and operation of PPB-based reactors. In pilot and full-scale systems, for example, process and environmental perturbation can influence the stability of the PPB community and wastewater treatment performance. Four short-term perturbations, likely to occur in a full-scale PPB system, were simulated to assess the effect of the perturbations on the model, namely as: (i) incoming VFA concentration (250, 500, and 3000 mgCODL<sup>-1</sup>d<sup>-1</sup>), (ii) incoming soluble organic matters (0, 100, and 3000 mgCODL<sup>-1</sup>d<sup>-1</sup>), (iii) incoming suspended solids (0, 250, 1000 mgCODL<sup>-1</sup>d<sup>-1</sup>), and (iv) the light intensity (14, 54, 108 W m<sup>-2</sup>). The simulation was run for 25 days at a 12 h light and 12 h dark condition and stirring regime of 12 h on and 12 h off to reach steady-state and the perturbations were, then, implemented.

### 3. Results and discussion

The lab-scale and even pilot-scale raceway reactors can be modelled as a single continuous-flow stirred tank (CSTR) due to their reduced dimensions and the high water circulation flow. Sequencing batch with cycles of filling the reactor with influent once a day and turning on the paddle wheel to promote gas transfer during the day, and stopping the paddle wheel to slow down the reactions and settle the biomass during nights prior to purging the excess sludge, was assumed as a modelling of the reactor regime to simulate the real situation in physical models in labs.

The average light intensity in the bioreactor was determined based on Lambert-Beer’s Law, which was formulated in the form of an inhibition function to differentiate light illumination between day and night. Light attenuation (Solimeno et al., 2017) was also taken into account in function of the biomass concentration to formulate a close-to-real-world condition for light intensity. The model is capable of simulating the process under real-world conditions by incorporating historical solar irradiation data as well as other operational scenarios with artificial lighting, as light intensity serves as an input parameter for the model’s implementation. In the following, the results are presented in three distinct sections: sensitivity analysis (Table 3), calibration and validation (Table 4), and perturbed scenario assessment (Figure 1).

#### 3.1. Sensitivity analysis

The sensitivity analysis revealed the influential parameters for further calibration. Maximal specific growth rates ( $\mu_m$ ), specific decay rates ( $b_m$ ) and kinetic parameters related to oxygen as well as light constants had the greatest impact on the PPB abundance. Substrate half-saturation constants ( $K_S$ ) such as the soluble organic for phototrophic and chemotrophic growth of PPB and VFA for chemotrophic and aerobic heterotrophic growth of PPB did not show any or only a very low impact (close to zero). Similar results have been also reported by Biase et al. (2021), for a high-rate moving bed biofilm reactor model, which showed that the aerobic decay rate and maximal specific growth rate of AEB had a 5–12 times stronger impact on the model compared to substrate half-saturation constants.

The effect of parameter variation on the model output was only impactful in a specific range, typically between 0.50–5.45 times the baseline values. Furthermore, the sensitivity analysis showed that the relative PPB abundance was more sensitive to parameter variations compared to the other model outputs. This is because of splitting PPB community and differentiating among light and oxygen inhibitions to build a model more accurate in terms of predicting PPB abundance. This also reflected the challenge to construct a model, which predicts relative PPB abundances.

The most impactful parameter is the maximal specific growth rate of aerobic chemoheterotrophic AEB ( $\mu_{m,SS,AEB}$ ), which directly affects the microbial community distribution and COD removal rates. Managing passive oxygen entry into a raceway reactor, especially during nighttime through paddle wheel control, can boost PPB abundance significantly.

Additionally, the maximal specific aerobic chemoheterotrophic growth rate of PPB on VFA ( $\mu_{m,VFA,PPB,aec}$ ) is essential for PPB to compete with AEB under

dark aerobic conditions. Parameters related to oxygen, such as the oxygen half-saturation constants ( $K_{S,O_2,PPB}$  and  $K_{S,O_2,AEB}$ ) and oxygen inhibitory constant for phototrophic growth of PPB ( $K_{I,O_2,PPB}$ ), also have a substantial impact, particularly in low dissolved oxygen raceway systems.

Furthermore, light-related parameters, including the light half-saturation constant of PPB ( $K_{S,E}$ ) and the light inhibitory constant for chemotrophic growth of PPB ( $K_{I,E}$ ), play a critical role. These parameters determine the balance between aerobic chemoheterotrophy and phototrophy in response to varying light intensities. A summary of sensitivity analysis is provided in Table 3.

Overall, the sensitivity analysis uncovered the impactful parameters of the PBM. Specifically the parameters  $K_{S,O_2,PPB}$ ,  $K_{I,O_2,PPB}$ ,  $K_{S,E}$ ,  $K_{I,E}$  and  $M_S$  are thus far unreported or only limited-studied, yet have a strong impact on the model. Therefore, the calibration of these five parameters and comparison of the simulated output with experimental data of a raceway reactor were presented in the following.

### 3.2. Calibration and validation

According to the sensitivity analysis, five impactful PPB-related parameters were identified that have not been described in literature and not yet calibrated for a raceway reactor, namely the oxygen half-saturation constant for aerobic chemoheterotrophic growth of PPB ( $K_{S,O_2,PPB}$ ), oxygen inhibitory constant for phototrophic growth of PPB ( $K_{I,O_2,PPB}$ ), light half-saturation constant of PPB ( $K_{S,E}$ ), light inhibitory constant for chemotrophic growth of PPB ( $K_{I,E}$ ) and the parallel metabolic growth factor ( $M_S$ ) that is newly introduced to the model.  $K_{I,O_2,PPB}$ ,  $K_{I,E}$ , and  $M_S$  have not been reported in literature, yet are crucial for the proper functioning of the model based on their impact on the PPB abundance and COD removal.

Model calibration combined with data of the three controlled experiments explained in “overview of experiments” section, resulted in a value for  $K_{S,O_2,PPB}$ ,  $K_{I,O_2,PPB}$ ,  $K_{S,E}$ ,  $K_{I,E}$  and  $M_S$  of  $0.05 \text{ mgO}_2\text{L}^{-1}$ ,  $5 \text{ mgO}_2\text{L}^{-1}$ ,  $4 \text{ W m}^{-2}$ ,  $135 \text{ W m}^{-2}$ , and 0.28, respectively. Overall, the simulated and experimental outputs are in good agreement and show a similar trend over the three operational strategies, based on the summarized results in Table 4. In terms of relative error, the model has predicted the third scenario of the experiments, i.e. the half-day light and half-day dark condition along with constantly stirring, more accurately than the other two. In terms of COD output accuracy, relative errors of COD removal rate, biomass productivity, and PPB abundance are in an acceptable range.

Two oxygen-PPB-related parameters were calibrated, namely the oxygen half-saturation constant for aerobic chemoheterotrophic growth of PPB ( $K_{S,O_2,PPB}$ ) and oxygen inhibitory constant for phototrophic growth of PPB ( $K_{I,O_2,PPB}$ ). The oxygen half-saturation constant was calibrated to  $0.05 \text{ mgO}_2\text{L}^{-1}$ , which is aligned with the oxygen half-saturation constant for AEB in the activated sludge model (Henze et al., 2015). The second oxygen-PPB-related parameter, i.e.  $K_{I,O_2,PPB}$ , is responsible for the direct oxygen suppression of the photoheterotrophic growth. A value of  $5 \text{ mgO}_2\text{L}^{-1}$  is assigned to the parameter after calibration. Calibrating the oxygen inhibitory constant through a dedicated experimental setup at different oxygen concentrations is challenging. PPB are able to grow both photo- and chemoheterotrophically. Increasing the dissolved oxygen concentration even results in an enhancement of the growth rate due to

additional chemoheterotrophic conversion, e.g. 10% increase in maximal specific growth rate subject to increase in oxygen transfer from 72 to 336 mgO<sub>2</sub>L<sup>-1</sup> (Alloul et al., 2021a). It should be highlighted that next to dissolved oxygen concentration, the oxygen transfer rate is also a key factor steering the microbial community in a raceway reactor. Together with the oxygen uptake rate, it influences the actual dissolved Oxygen concentration in the system.

Two light-related parameters, i.e.  $K_{S,E}$  and  $K_{I,E}$  were also calibrated. The calibrated value of  $K_{I,E}$  is 4 W m<sup>-2</sup>, in the range (i.e. 4.58±7.40 W m<sup>-2</sup>) reported by Capson-Tojo et al. (2022). In comparison with other work and their experiments such as Capson-Tojo et al. (2022); Katsuda et al. (2000), it can be concluded that different wavelengths and inoculum result in other type of pigment responsible for light capturing, which might also affect the effective the light half-saturation constant. The second calibrated light-related parameter of the model inhibits the (an)aerobic chemoheterotrophic growth of PPB. Along with  $K_{I,O_2,PB}$ , it enables the PPB community to allocate their metabolic growth pathway between photo- and chemoheterotrophy.

The parallel metabolic growth factor ( $M_S$ ) as the final parameter considered for calibration, allows PPB to account different metabolisms in parallel. The final calibrated value was assigned to 0.28. This suggests that the PPB growth in a raceway reactor is probably not governed by independent subpopulations, however individual PPB cells may switch between metabolism. The experiments done by Alloul et al. (2021b) showed that the PPB species *Rhodobacter capsulatus*, *Rb. sphaeroides*, *Rhodopseudomonas palustris* and *Rhodospirillum rubrum* are able to switch from photoheterotrophy to aerobic chemoheterotrophy and from photoheterotrophy to photoautotrophy, which supports the idea of integrating the metabolic constant to the PBM.

### 3.3. Perturbed scenario assessment

The effect of process and environmental perturbations, which are likely-to-occur in pilot- and full-scale raceway systems, was assessed with respect to the stability of the PPB community. Four different perturbation scenarios, as described, were simulated and the results were depicted in Figure 1. The fluctuations observed in the curves represent daily variations in PPB abundance. PPB are produced through both photoheterotrophic and aerobic and anaerobic chemoheterotrophic processes. In the context of an open reactor, the contribution of anaerobic chemoheterotrophic growth to PPB abundance is minimal. Instead, the primary metabolic pathway for PPB growth is through photoheterotrophy. This growth steadily increases when exposed to solar radiation and decreases in the absence of light, that causes daily fluctuation in PPB abundance.

The wastewater composition can change throughout the day. The effect of influent VFA variability (500–3000 mg COD L<sup>-1</sup>) was, therefore, assessed on the model performance. This scenario is depicted in Figure 1 (A) showing that the PPB abundance is immediately affected when the incoming VFA concentration drops from 3000 to 500 mg COD L<sup>-1</sup>. When organic carbon is limited in the reactor, dissolved oxygen can freely increase up to 3 mgO<sub>2</sub>L<sup>-1</sup>. This oxygen increase eventually inhibits the phototrophic growth of PPB. Lowering the HRT and, thus, increasing the volumetric loading rate can be a contingency measure, yet the raceway reactor is typically designed for a certain range in flow rate. Increasing the SRT is a better solution as it increases the retention of PPB in

the system, thereby, lowering the impact of oxygen inhibition. The increase in oxygen still occurs, yet PPB is less heavily affected. A faster contingency strategy would be decreasing paddle wheel rotation or even stopping it completely. An oxygen sensor with paddle wheel speed control can help to steer the oxygen transfer to the system to cope with changes in loading rates during operation.

The second perturbation considered the effect of soluble organic matters (non-VFA matters) in the incoming wastewater ( $0\text{--}3000\text{ mg COD L}^{-1}$ ) as depicted in Figure 1 (B). For PPB systems, several articles recommended to preferment the wastewater, thereby, separating acidogenic fermentation and PPB biomass production (Alloul et al., 2021a, 2018; Cerruti et al., 2023). This would result in lower competition with acidogenic fermentative microorganisms and provides more accessible organic carbon in the form of VFA for PPB to grow. PPB are also able to ferment, yet their maximal specific anaerobic chemoheterotrophic growth rate is lower compared to non-PPB, i.e.  $0.3$  vs  $0.6\text{ d}^{-1}$  (Alloul et al., 2021a). For instance, PPB cannot compete with acidogenic fermenters on sucrose-rich synthetic wastewater (Cerruti et al., 2023). The perturbations reconfirmed these experimental observations as shown in Figure 1(B), in which a drop in relative PPB abundance from 30 % to 11 % when the wastewater composition changes from 100 % VFA to 100 % non-VFA.

The third perturbation simulated variations in influent suspended solids. These organics can cause higher turbidity of the water and, thereby, lower the light availability for phototrophs and less PPB abundance as depicted in Figure 1 (C). Suspended solids concentrations as low as  $250\text{ mg COD L}^{-1}$  drops the PPB abundance from 26 % to 18 %. Suspended solids concentrations of  $1000\text{ mg COD L}^{-1}$  resulted in a complete collapse of the PPB community. In this case, stopping the feed and operate the reactor in semi-continuous mode until full recovery achieved again would be a solution. The results also showed that a good solid/liquid separation is crucial to prevent suspended material from entering the raceway reactor.

Light intensity was the last studied perturbation. The results again showed a serious disruption on the PPB community, as depicted in Figure 1 (D). As expected, variations of light intensity had an important impact on the stability of the phototrophic community; when the light intensity decreases from  $108$  to  $14\text{ W m}^{-2}$  for 10 days, the final PPB abundance decreases from 27 % to 7 %.

The effect of SRT and HRT on the PPB abundance and the treatment performance is also crucial, particularly SRT that can cope with sudden perturbations that may destabilize the reactor performance as a contingency measure. The extension of the SRT would minimize the effect of TSS in influent to increase the PPB abundance, while increasing the COD removal efficiency. For an incoming concentration of  $3000\text{ mg COD L}^{-1}$ , an SRT between 3–4 d can be chosen to minimally reach a COD removal efficiency of 60 %, considering HRT between 3–4 d. Higher COD removal efficiencies up to 100 % are achievable for SRT and HRT, with less HRT compared to SRT. The related figure to the effect of SRT and HRT on the PPB abundance and the treatment performance can be found in the supplementary material (see supplementary material).

#### *3.4. Model implications and further development*

To reduce the multiscale complexity of the PBM, simplifications on metabolisms that PPB can adopt in nature were made. For instance, photolithoautotrophic growth by PPB on carbon dioxide as a carbon source and dihydrogen or iron

H as electron donors, and  $N_2$ -fixation by PPB were not included. These latter metabolisms are less likely to occur in the raceway reactor. However, depending on local conditions to be studied, the PBM structure can be adapted. Species or strain specific metabolic traits of PPB such as denitrification, and autotrophic uptake of hydrogen were also not adopted in the model for the sake of simplicity and the type of raceway reactor.

For further modelling improvement, other PPB metabolisms and microbial community can be included, considering losing simplicity for simulation application to increasing accuracy for detailed biological analysis. The integration of temperature dependency and dynamic pH of the biological and other physical processes can also be added depending on an operational condition under consideration, since the temperature and pH were considered to be fixed in the PBM.

This model is primarily focused on offering a mechanistic framework within the realm of modelling to elucidate a specific observation derived from previously reported experimental studies. Since PBM is a new mechanistic model for PPB community in terms of metabolic-mechanistic understanding, the transfer of biotechnology from a proof-of-concept to practical application requires a proof-of-feasibility. Calibrating and verifying the model under various conditions and configurations would enable expanding its applicability and accuracy by designing some dedicated experiments for different metabolisms. Additionally, kinetic parameters can also be experimentally estimated using different substrates and light ranges, considering a dominant metabolic growth pathway alongside different simultaneous potential growth ways, in which more experiments should be carried out to evaluate these options as a future research.

#### 4. Conclusions

In this paper, a new mechanistic model to describe the mechanisms of microbial selection, competition and conversions in an open raceway reactor was proposed. The model integrates three different metabolisms of PPB, and competing aerobic and anaerobic organisms that can prevail in a raceway reactor. Integration of parallel metabolic growth was modelled. The model was shown to be able to accurately predict changes in the PPB abundance and COD removal rates with the relative errors 19.5 % and 12 %, respectively. The outputs of the simulated perturbation scenarios were shown to capture both theoretical understanding and experimental observations of PPB-based processes.

##### **Appendix A. Supplementary material**

Supplementary material of this work can be found in online version of the paper.

#### References

- Acién, F., Fernández, J., Magán, J., Molina, E., 2012. Production cost of a real microalgae production plant and strategies to reduce it. *Biotechnology Advances* 30, 1344–1353.
- Alloul, A., Blansaer, N., Segura, P.C., Wattiez, R., Vlaeminck, S.E., Leroy, B., 2023. Dehazing redox homeostasis to foster purple bacteria biotechnology. *Trends in Biotechnology* 41, 106–119.

- Alloul, A., Cerruti, M., Adamczyk, D., Weissbrodt, D.G., Vlaeminck, S.E., 2021a. Operational strategies to selectively produce purple bacteria for microbial protein in raceway reactors. *Environmental Science & Technology* 55, 8278–8286.
- Alloul, A., Ganigué, R., Spiller, M., Meerburg, F., Cagnetta, C., Rabaey, K., Vlaeminck, S.E., 2018. Capture–ferment–upgrade: A three-step approach for the valorization of sewage organics as commodities. *Environmental Science & Technology* 52, 6729–6742.
- Alloul, A., Muys, M., Hertoghs, N., Kerckhof, F.M., Vlaeminck, S.E., 2021b. Cocultivating aerobic heterotrophs and purple bacteria for microbial protein in sequential photo- and chemotrophic reactors. *Bioresource Technology* 319, 124192.
- Batstone, D., Keller, J., Angelidaki, I., Kalyuzhnyi, S., Pavlostathis, S., Rozzi, A., Sanders, W., Siegrist, H., Vavilin, V., 2002. The IWA anaerobic digestion model no 1 (ADM1). *Water Science and Technology* 45, 65–73.
- Biase, A., Kowalski, M.S., Devlin, T.R., Oleszkiewicz, J.A., 2021. Modeling of the attached and suspended biomass fractions in a moving bed biofilm reactor. *Chemosphere* 275, 129937.
- Capson-Tojo, G., Batstone, D.J., Grassino, M., Hülsen, T., 2022. Light attenuation in enriched purple phototrophic bacteria cultures: Implications for modelling and reactor design. *Water Research* 219, 118572.
- Capson-Tojo, G., Batstone, D.J., Grassino, M., Vlaeminck, S.E., Puyol, D., Verstraete, W., Kleerebezem, R., Oehmen, A., Ghimire, A., Pikaar, I., Lema, J.M., Hülsen, T., 2020. Purple phototrophic bacteria for resource recovery: Challenges and opportunities. *Biotechnology Advances* 43, 107567.
- Capson-Tojo, G., Batstone, D.J., Hülsen, T., 2023. Expanding mechanistic models to represent purple phototrophic bacteria enriched cultures growing outdoors. *Water Research* 229, 119401.
- Capson-Tojo, G., Lin, S., Batstone, D.J., Hülsen, T., 2021. Purple phototrophic bacteria are outcompeted by aerobic heterotrophs in the presence of oxygen. *Water Research* 194, 116941.
- Casagli, F., Zuccaro, G., Bernard, O., Steyer, J.P., Ficara, E., 2021. ALBA: A comprehensive growth model to optimize algae-bacteria wastewater treatment in raceway ponds. *Water Research* 190, 116734.
- Cerruti, M., Crosset-Perrotin, G., Ananth, M., Rombouts, J.L., Weissbrodt, D.G., 2023. Syntrophy between fermentative and purple phototrophic bacteria to treat and valorize carbohydrate-rich wastewaters. *Bioresource Technology Reports* , 101348.
- Cerruti, M., Stevens, B., Ebrahimi, S., Alloul, A., Vlaeminck, S.E., Weissbrodt, D.G., 2020. Enrichment and aggregation of purple non-sulfur bacteria in a mixed-culture sequencing-batch photobioreactor for biological nutrient removal from wastewater. *Frontiers in Bioengineering and Biotechnology* 8.

- Golomysova, A., Gomelsky, M., Ivanov, P.S., 2010. Flux balance analysis of photoheterotrophic growth of purple nonsulfur bacteria relevant to biohydrogen production. *International Journal of Hydrogen Energy* 35, 12751–12760.
- Henze, M., Gujer, W., Mino, T., van Loosedrecht, M., 2015. Activated sludge models ASM1, ASM2, ASM2d and ASM3. *Water Intelligence Online* 5.
- Hülßen, T., Züger, C., Gan, Z.M., Batstone, D.J., Solley, D., Ochre, P., Porter, B., Capson-Tojo, G., 2022. Outdoor demonstration-scale flat plate photobioreactor for resource recovery with purple phototrophic bacteria. *Water Research* 216, 118327.
- Imam, S., Yilmaz, S., Sohmen, U., Gorzalski, A.S., Reed, J.L., Noguera, D.R., Donohue, T.J., 2011. iRsp1095: A genome-scale reconstruction of the rhodobacter sphaeroides metabolic network. *BMC Systems Biology* 5.
- Imhoff, J., 2006. The phototrophic alpha-proteobacteria. prokaryotes: a handbook on the biology of bacteria, vol 5: Proteobacteria: alpha and beta subclasses. Springer, New York. doi 10, 0–387.
- Katsuda, T., Arimoto, T., Igarashi, K., Azuma, M., Kato, J., Takakuwa, S., Ooshima, H., 2000. Light intensity distribution in the externally illuminated cylindrical photo-bioreactor and its application to hydrogen production by rhodobacter capsulatus. *Biochemical Engineering Journal* 5, 157–164.
- Manhaeghe, D., Blomme, T., Hulle, S.V., Rousseau, D., 2020. Experimental assessment and mathematical modelling of the growth of chlorella vulgaris under photoautotrophic, heterotrophic and mixotrophic conditions. *Water Research* 184, 116152.
- Norsker, N.H., Barbosa, M.J., Vermuë, M.H., Wijffels, R.H., 2011. Microalgal production — a close look at the economics. *Biotechnology Advances* 29, 24–27.
- Puyol, D., Barry, E., Hülßen, T., Batstone, D., 2017. A mechanistic model for anaerobic phototrophs in domestic wastewater applications: Photo-anaerobic model (PANM). *Water Research* 116, 241–253.
- Solimeno, A., Acien, F.G., García, J., 2017. Mechanistic model for design, analysis, operation and control of microalgae cultures: Calibration and application to tubular photobioreactors. *Algal Research* 21, 236–246.

Figure 1: Effects of the perturbation scenarios on relative PPB abundance based on variations on (A) influent VFA (250, 500, and 3000 mg COD L<sup>-1</sup>), (B) influent soluble organic (non-VFA) (0, 100, and 3000 mg COD L<sup>-1</sup>), (C) influent suspended solid (0, 250, and 1000 mg COD L<sup>-1</sup>), and (D) light (14, 54, and 108 W m<sup>-2</sup>). The perturbation was applied on day 25.

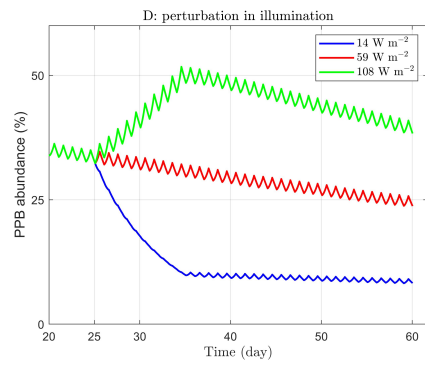
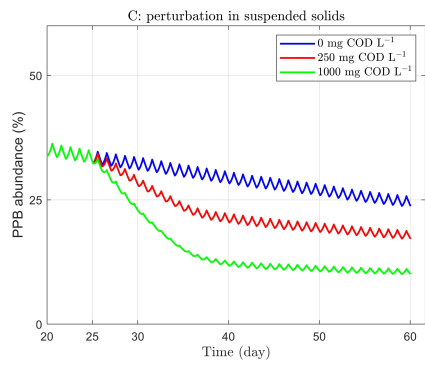
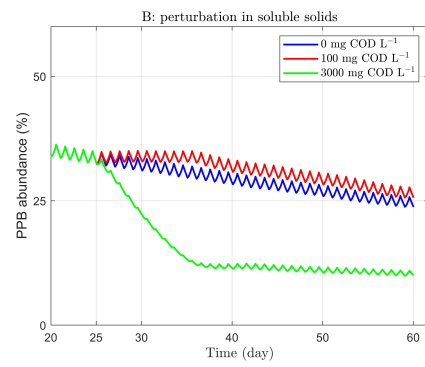
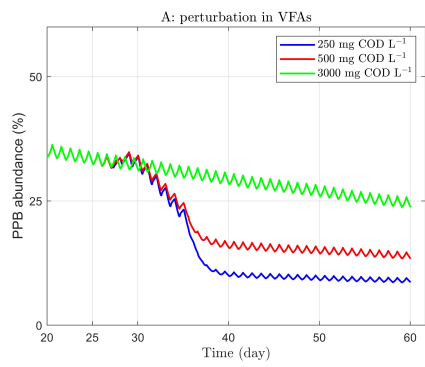


Table 1: State variables included in the PBM categorized in a particulate ( $X$ ) and soluble ( $S$ ) fraction. Microbial biomass in forms of purple phototrophic bacteria (indexed by PB), aerobic bacteria (AEB) and anaerobic bacteria (ANB). PPB can be grown photoheterotrophically (ph), aerobic chemoheterotrophically (aec), and anaerobic chemoheterotrophically (anc).

<b>Symbol</b>	<b>Description</b>	<b>Unit</b>
<b>Microbial biomass</b>		
$X_{PB,ph}$	Photoheterotropic grown PPB	mg COD L <sup>-1</sup>
$X_{PB,aec}$	Aerobic chemoheterotropic grown PPB	mg COD L <sup>-1</sup>
$X_{PB,anc}$	Anaerobic chemoheterotropic grown PPB	mg COD L <sup>-1</sup>
$X_{AEB}$	Aerobic bacteria	mg COD L <sup>-1</sup>
$X_{ANB}$	Anaerobic bacteria	mg COD L <sup>-1</sup>
<b>Substrates and products</b>		
$X_S$	Slowly biodegradable organic matter	mg COD L <sup>-1</sup>
$X_I$	Inert particulate organic matter	mg COD L <sup>-1</sup>
$S_S$	Readily biodegradable organic matter	mg COD L <sup>-1</sup>
$S_{VFA}$	Volatile fatty acids	mg COD L <sup>-1</sup>
$S_I$	Inert soluble organic matter	mg COD L <sup>-1</sup>
$S_{H2}$	Soluble hydrogen	mg COD L <sup>-1</sup>
$S_{IC}$	Total inorganic carbon	mmolHCO <sub>3</sub> <sup>-</sup> L <sup>-1</sup>
$S_{IN}$	Total inorganic nitrogen	mgNL <sup>-1</sup>
$S_{IP}$	Total inorganic phosphorus	mgPL <sup>-1</sup>
$S_{O2}$	Dissolved oxygen	mgO <sub>2</sub> L <sup>-1</sup>

Table 2: Biological and physical process rates in the PBM model.

$\rho(\cdot)$	Description	Rate equation
<b>Purple bacteria (<math>X_{PB}</math>)</b>		
1	Photoheterotrophic growth on soluble organics such as carbohydrates and alcohols (excluding VFA).	$\mu_{m,SS,PB,ph} \frac{S_E}{S_E+K_{I,E}} \frac{K_{I,O2,PB}}{K_I} \frac{S_{IN}}{S_{IN}+K_{S,IN}} \frac{S_{IP}}{S_{IP}+K_{S,IP}} \frac{S_S}{S_S+K_{S,SS,ph}} f_{ph}(X_{PB}, M_S)$
2	Photoheterotrophic growth on VFA. The main products are biomass and carbon dioxide.	$\mu_{m,VFA,PB,ph} \frac{K_{I,E}}{K_I} \frac{S_{O2,PB}}{S_{O2}+K_{I,E}} \frac{S_{IN}}{S_{IN}+K_{S,IN}} \frac{S_{IP}}{S_{IP}+K_{S,IP}} \frac{S_S}{S_S+K_{S,SS,ph}} f_{ph}(X_{PB}, M_S)$
3	Aerobic chemoheterotrophic growth on soluble organics with oxygen as terminal electron acceptor.	$\mu_{m,SS,PB,acc} \frac{K_{S,E}}{K_S} \frac{S_{O2,PB}}{S_{O2}+K_{S,E}} \frac{S_{IN}}{S_{IN}+K_{S,IN}} \frac{S_{IP}}{S_{IP}+K_{S,IP}} \frac{S_S}{S_S+K_{S,SS,acc}} f_{acc}(X_{PB}, M_S)$
4	Aerobic chemoheterotrophic growth on VFA.	$\mu_{m,VFA,PB,acc} \frac{K_{S,E}}{K_S} \frac{S_{O2,PB}}{S_{O2}+K_{S,E}} \frac{S_{IN}}{S_{IN}+K_{S,IN}} \frac{S_{IP}}{S_{IP}+K_{S,IP}} \frac{S_S}{S_S+K_{S,SS,acc}} f_{acc}(X_{PB}, M_S)$
5	Anaerobic chemoheterotrophic growth and acidogenic fermentation reactions on soluble organics. The main products are biomass, hydrogen, carbon dioxide and VFA.	$\mu_{m,SS,PB,anc} \frac{K_{S,E}}{K_S} \frac{S_{O2,PB}}{S_{O2}+K_{S,E}} \frac{S_{IN}}{S_{IN}+K_{S,IN}} \frac{S_{IP}}{S_{IP}+K_{S,IP}} \frac{S_S}{S_S+K_{S,SS,anc}} f_{anc}(X_{PB}, M_S)$
6	Decay of PPB biomass into biodegradable ( $X_S$ ) and inert ( $X_I$ ) organic matter and release of ammonium, phosphate, and bicarbonate.	$b_{m,PB,dec}(X_{PB,ph} + X_{PB,anc})$
<b>Aerobic bacteria (<math>X_{AEB}</math>)</b>		
7	Aerobic chemoheterotrophic growth on soluble organics with oxygen as terminal electron acceptor.	$\mu_{m,SS,AEB} \frac{K_{S,O2,acc}}{K_{S,O2}} \frac{S_{IN}}{S_{IN}+K_{S,IN}} \frac{S_{IP}}{S_{IP}+K_{S,IP}} \frac{S_S}{S_S+K_{S,SS,AEB}} \frac{X_{AEB}}{X_{AEB}}$
8	Aerobic chemoheterotrophic growth on VFA.	$\mu_{m,VFA,AEB} \frac{K_{S,O2,acc}}{K_{S,O2}} \frac{S_{IN}}{S_{IN}+K_{S,IN}} \frac{S_{IP}}{S_{IP}+K_{S,IP}} \frac{S_S}{S_S+K_{S,SS,AEB}} \frac{X_{AEB}}{X_{AEB}}$
9	Decay of AEB biomass into biodegradable ( $X_S$ ) and inert ( $X_I$ ) organic matter and release of ammonium, phosphate, and bicarbonate.	$b_{m,AEB,dec} X_{AEB}$
<b>Anaerobic bacteria (<math>X_{ANB}</math>)</b>		
10	Anaerobic chemoheterotrophic growth and acidogenic fermentation reactions on soluble organics. The main products are biomass, hydrogen, carbon dioxide and VFA.	$\mu_{m,VFA,ANB} \frac{K_{S,O2,ANB}}{K_{S,O2}+K_{S,O2,acc,ANB}} \frac{S_{IN}}{S_{IN}+K_{S,IN}} \frac{S_{IP}}{S_{IP}+K_{S,IP}} \frac{S_S}{S_S+K_{S,SS,ANB}} X_{ANB}$
11	Decay of ANB biomass into biodegradable ( $X_S$ ) and inert ( $X_I$ ) organic matter and release of ammonium, phosphate, and bicarbonate.	$b_{m,ANB,dec} X_{ANB}$
<b>Hydrolysis</b>		
12	Hydrolysis of biodegradable particulates ( $X_S$ ) into soluble ( $S_S$ and $S_{VFA}$ ) and inert organic carbon ( $X_I$ ), ammonium, hydrogen and bicarbonate.	$\mu_{hyd} X_S$
<b>Physical processes</b>		
13	Stripping/dissolution of oxygen in raceway reactor.	$K_{laO2}(O_2^{sat} - S_{O2})$
14	Stripping/dissolution of carbon dioxide in raceway reactor.	$K_{laCO2}(CO_2^{sat} - S_{O2})$
15	Stripping of hydrogen in raceway reactor.	$K_{laH2}(H_2^{sat} - S_{H2})$
16	Stripping of ammonium in raceway reactor.	$K_{laNH3}(NH_3^{sat} - S_{NH3})$

Table 3: Sensitivity analysis of the most impactful kinetic parameters of the PBM. Sensitivity analysis is computed by changing the default value of each parameter one by one, ten times higher and lower, while keeping the other parameters constant. The mean for the PPB abundance, chemical oxygen demand (COD) removal rate (mg COD removed  $L^{-1} d^{-1}$ ), biomass productivity (mg COD biomass  $d^{-1}$ ) and the biomass yield (mg COD biomass mgCODremoved) of the last five days for each iteration is calculated and divided by the output results of the baseline (default values) to obtain the relative error.

Parameter (unit)	Symbol	Default	Impact on			
			PPB abundance	COD removal	Biomass productivity	Biomass yield
Parallel metabolic growth (-)	$M_S$	0.300	13.98	0.33	1.72	-0.74
Maximal specific of AEB on soluble organics ( $d^{-1}$ )	$\mu_{m,SS,AEB}$	0.076	-10.97	-10.97	-2.24	0.04
Maximal specific aerobic chemotrophic growth rate of PPB on volatile fatty acids ( $d^{-1}$ )	$\mu_{m,VFA,AEB}$	0.053	10.94	-10.94	-0.60	0.07
Specific decay rate of PPB ( $d^{-1}$ )	$b_{m,PB,dec}$	0.011	-10.11	-10.11	-2.29	0.54
Oxygen half-saturation constant for chemotrophic growth of PPB ( $mgO_2L^{-1}$ )	$K_{S,O_2,PB}$	0.050	-9.92	-9.92	0.53	-0.08
Maximal specific phototrophic growth rate of AEB ( $mgO_2L^{-1}$ )	$\mu_{m,VFA,PB,ph}$	0.078	9.90	9.90	2.09	-0.93
Oxygen half-saturation constant for AEB ( $mgO_2L^{-1}$ )	$K_{S,O_2,AEB}$	0.050	-9.26	-9.26	-0.50	-0.06
Specific decay rate of AEB ( $mgO_2L^{-1}$ )	$b_{m,AEB,dec}$	0.016	8.99	8.99	0.49	-0.06
Light half-saturation constant of PPB ( $W m^{-2}$ )	$K_{S,E}$	4.500	-7.44	-7.44	0.39	2.29
Maximal specific aerobic chemotrophic growth rate of PPB on soluble organics ( $d^{-1}$ )	$\mu_{m,SS,PB,acc}$	0.050	2.87	2.87	-0.16	-0.03
Maximal specific anaerobic chemotrophic growth rate of PPB on soluble organics ( $d^{-1}$ )	$\mu_{m,SS,PB,anc}$	0.012	2.36	0.14	-0.13	0.07
Light inhibitory constant for chemotrophic growth of PPB ( $W m^{-2}$ )	$K_{I,E}$	200.000	1.40	1.40	-0.09	-0.02
Maximal specific phototrophic growth rate of PPB on soluble organics ( $d^{-1}$ )	$\mu_{m,SS,PB,ph}$	0.053	1.31	1.31	-0.07	0.04
Oxygen inhibitory constant for phototrophic growth of PPB ( $mgO_2L^{-1}$ )	$K_{I,O_2,PB}$	5.000	1.20	0.00	-0.08	-0.02

Table 4: Calibration results including calibrated model outputs for relative purple phototrophic bacteria abundance, chemical oxygen demand (COD) removal rate, biomass productivity, and biomass yield and associated experimental data for three defined operational scenarios. Mean relative errors for the scenarios as well as mean relative errors for the selected outputs are also provided.

Scenario	Experiment and simulation conditions		Purple bacteria (Relative abundance %)		COD removal rate (mgCODL <sup>-1</sup> )		Biomass productivity (mgCODL <sup>-1</sup> )		Biomass yield (mg COD <sub>biomass</sub> mg <sup>-1</sup> COD <sub>removed</sub> )		Relative error (↓)
	Illumination (hg/ht/dark)	Stirring (on/off)	Surface-to-volume (m <sup>2</sup> m <sup>-3</sup> )	Experiment	Model	Experiment	Model	Experiment	Model	Experiment	
1	12h/12h	24h on	5	14	721.83	702.66	0.45	0.64	326	459	21.83
2	12h/12h	12h/12h	5	27	462.50	593.52	0.65	0.62	302	390	26.04
3	12h/12h	24h on	10	90	785.17	822.31	0.58	0.53	452	577	14.08
Relative error (→)				19.50	11.90		18.57		32.62		-